

A Comparative Analysis of BER Performance for NOMA in the Presence of Rayleigh Fading and Impulse Noise

Muhammad Hussain¹, Hina Shakir¹, Qamar Ud Din Memon¹, Taimoor Zafar² and Muhammad Zohaib Sohail²

¹Software Engineering Department, Bahria University, Karachi, Pakistan

²Electrical Engineering Department, Bahria University, Karachi, Pakistan

***Correspondence:** Muhammad Hussain, enr.m.hussain.bukc@bahria.edu.pk

Citation | Hussain. M, Shakir. H, Memon. Q. U, Zafar. T, Sohail. M. Z, "A Comparative Analysis of BER Performance for NOMA in the Presence of Rayleigh Fading and Impulse Noise", IJIST, Vol. 6 Issue. 2 pp. 550-564, May 2024

DOI | <https://doi.org/10.33411/ijist/202462550564>

Received | May 08, 2024 **Revised |** May 15, 2024 **Accepted |** May 21, 2024 **Published |** May 28, 2024.

Importance of Study: This research investigates the integration of wired and wireless communication in Smart Grid (SG) systems, addressing the challenges posed by impulse noise and the increasing demand for bandwidth.

Novelty statement: The study explores the impact of impulse noise models on Non-Orthogonal Multiple Access (NOMA) performance within fading environments, offering insights into optimizing bandwidth utilization in multi-user SG communication.

Material and Method: Numerical simulations validate the derived closed form of the bit error rate (BER) equation, utilizing a NOMA downlink system. The performance parameters for assessing the effects of impulse noise in a Rayleigh fading channel include instantaneous signal-to-noise ratio (SNR), bit error rate, disturbance ratio, and the trade-off between spectral efficiency and energy efficiency.

Result and Discussion: The research reveals that NOMA demonstrates promising performance in SG communication despite the presence of impulse noise, with BER decreasing rapidly with increasing signal-to-noise ratio (SNR). The study highlights a performance trade-off between impulse noise and fading, emphasizing the importance of accurate SNR levels for power allocation in NOMA systems.

Concluding Remarks: This study contributes novel insights into the robustness of NOMA under realistic SG conditions, offering valuable implications for enhancing reliability and efficiency in SG communication infrastructure.

Keywords: Smart Grid (SG), Smart Meter (SM), Non-orthogonal Multiple Access (NOMA), Power Division Multiple Access (PDMA) and Successive Interference Cancellation (SIC).



Introduction:

The key attributes of smart power grids are fusion of computation, networking, and physical processes requiring a control system, wireless devices, and a bi-directional communication network that attaches consumers and power utility. Smart Grid (SG) has facilitated domestic consumers by introducing an Advanced Metering Infrastructure (AMI) which receives, stores, and processes information from Smart Meters (SMs) and sends it to the smart power control and management system. SG aims to connect all the entities through communications while improving performance without using traditional approaches. Controllability, observability, and fast reliable information flow, over an efficient communication system is pivotal for a safe, reliable, and secure power grid. The essential part of SG communication is a wireless technology that links directly to the supply company to consumers because it is very costly to develop wired networks to observe several connections with diverse interfaces. Since numerous constraints are required to be examined in the grid, wired networks can result in complicated and costly communication architecture, necessitating a careful examination of constraints within the grid [1][2].

A conventional electrical meter is limited to measure the total utilization of energy in homes or offices etc. In contrast, in-home display SMs can collect previous and on-time energy usage parameters to manage energy consumption. Power utilities leverage this data to enhance their energy management systems, gathering insights into usage patterns during peak and off-peak hours, power factors, line losses, and instances of power theft. Transducers are usually connected to the power line to measure the energy parameters that are visible to the user by SM's display and are transmitted to power companies through the communication unit of SM. However, challenges in the electrical system, impact the communication network and degrades the performance of the communication unit of SM, introducing noise into Smart Grid (SG) communication networks. This research presents modeling and analysis of impulse noise which could be used for noise prediction and mitigation to improve the performance of the proposed communication infrastructure of SG [3][4].

Non-Orthogonal Multiple Access:

The wireless communication technologies employed in Home Area Network (HAN) and Building Area Network (BAN) in SG are Bluetooth, ZigBee, Wi-Fi. Although GSM, CDMA, WCDMA, and UMTS have sufficient bandwidth, these technologies are not capable of handling huge volumes of data generated by NAN and WAN through SG applications. A new emerging 5G technology known as the Non-Orthogonal Multiple Access (NOMA) scheme can fulfill the increasing demand for bandwidth in SG. NOMA has high spectral efficiency, as it allocates the entire bandwidth to every user at the same frequency and time, and differentiates users by allocating different power. In NOMA, users farther from the Base Station (BS) receive higher power than those who are closer, optimizing resource utilization. The Base Station (BS) superimposes signals of all users at the same time and frequency before transmission at the transmitter side. The BS combines signals from all users before transmission, with closer users employing Successive Interference Cancellation (SIC) to extract their own signals, while farther users' signals contribute significantly to the received signal, reducing the need for SIC. NOMA utilizes the strengths of varying distances of users from BS in order to allocate suitable power to the SMs that are installed at different distances [5][6].

The investigation of the impact of impulse noise on Non-Orthogonal Multiple Access (NOMA) in smart grid communication systems is driven by several pivotal factors. Firstly, it is highly relevant to smart grid communication, which is integral to modernizing energy distribution networks. As smart grids become increasingly prevalent, understanding the effects of impulse noise on communication systems is essential for ensuring their reliability and effectiveness in facilitating functions such as real-time monitoring and demand response. Secondly, impulse noise, particularly at smart meters, poses a significant practical challenge due

to the high-voltage environment. Investigating how impulse noise affects NOMA, a promising communication scheme, is crucial for developing robust and resilient smart grid communication solutions. Lastly, given the bandwidth demands of smart grid applications, NOMA offers a potential solution to meet these requirements. Therefore, understanding its performance in the presence of impulse noise is vital for optimizing bandwidth utilization and ensuring efficient communication in smart grids [4][5].

The findings of this research hold several practical applications with significant implications. Firstly, the research can inform strategies to mitigate the impact of impulse noise on NOMA performance, thereby enhancing the reliability and efficiency of smart grid communication systems. This optimization can lead to more reliable energy distribution, reduced downtime, and improved grid resilience. Additionally, the findings can guide the design and implementation of communication systems in smart grids, allowing engineers and designers to incorporate strategies for mitigating impulse noise effects into their designs. Moreover, policymakers and standardization bodies can utilize these findings to develop regulations and standards for smart grid communication systems, ensuring that reliability and performance requirements are met. Overall, the research addresses a critical challenge in modern energy distribution networks and has broad applications for improving grid reliability, efficiency, and resilience.

Motivation:

The deployment of a comprehensive communication infrastructure within the smart grid (SG) network presents a formidable challenge due to its vast and intricate nature. The SG ecosystem encompasses a diverse array of networks and environments, each with unique communication requirements and complexities. Key challenges faced in enabling effective communication within the SG framework include the need for scalable technology solutions to handle the instantaneous data transmission demands across various network types. Additionally, as the number of interconnected devices continues to grow, a spectrally efficient multiple access scheme is essential to manage the increasing data traffic efficiently. Ensuring electrically efficient and energy harvesting transmission methods becomes critical, especially for remote areas hosting sensors and actuators vital to the SG's functioning. Furthermore, modeling and analyzing the impact of impulse noise are paramount for implementing Smart Meters (SMs) and other communication devices seamlessly integrated within the power system. The communication challenges extend to urban areas as well, where fading environments must be considered for robust SG communication. Lastly, the measurement and standardization of technology implemented within the SG are crucial aspects that require thorough investigation and evaluation to ensure interoperability and optimal performance across the network. Addressing these challenges is fundamental to establishing a resilient and efficient communication infrastructure that underpins the transformative capabilities of the smart grid in modernizing energy distribution and management systems [7].

Objective:

This research comprises of following objectives:

- Modeling the impulse noise in SG environments.
- Analyzing the performance of NOMA systems under the influence of impulsive noise.
- To calculate the BER for the NOMA system in the presence of impulsive noise.
- To evaluate the reliability and effectiveness of the proposed NOMA-based communication model under realistic conditions.

The study presents a novel examination of the performance of NOMA systems within smart grid SG communication frameworks, particularly under the influence of Rayleigh fading and impulse noise. This research uniquely addresses the critical challenge of integrating NOMA with SG applications, a domain where traditional OFDMA methods often fall short in handling the increasing bandwidth demands and noise interference. By developing detailed models and

deriving closed-form equations for BER and SNR in these complex environments, the study offers significant insights into optimizing spectral and energy efficiency. The innovative approach of assessing NOMA's resilience against impulse noise provides a substantial contribution to the field, enhancing the reliability and efficiency of smart grid communications and offering practical solutions for noise prediction and mitigation.

Contribution:

In this research study, a communication infrastructure for SG, considering the main requirements and constraints is proposed. The contributions are:

- A NOMA scheme is proposed to provide high spectral efficiency to fulfill the bandwidth requirement of SG. Implementation of NOMA is suitable for static users because the change in distance of the user from BS can affect the received power of the user and NOMA differentiates users' signal based on power allocation.
- Utilization of the non-orthogonality of the proposed NOMA scaled for different types of networks and data requirements, since NOMA offers electrically efficient and energy harvesting transmission which is suitable for remote area sensors and actuators.
- Models for analyzing the effect of impulse noise on SMs are presented and an equation for instantaneous SNR is derived considering Rayleigh fading channel.
- The closed-form equation of BER is derived to measure the performance of the proposed model in the presence of fading and impulse noise.
- The effect of impulse noise on spectral and energy efficiency trade-off is analyzed and compared with existing technology, namely the Orthogonal Frequency Division Multiple Access (OFDMA) scheme.

The remaining part of the paper is organized as follows. A comprehensive review of the implementation of wireless communication in SG is presented in Section II, Noise modeling and the proposed system model are presented in section III and, in the end, we have summarized the article in Section V.

Literature Review:

The transition from a conventional power grid to a smart grid, especially in terms of communication infrastructure, remains a continuous endeavor due to the absence of efficient wired or wireless technologies. A document published by the National Institute of Standards and Technology (NIST) has presented a general review of some wired and wireless communication technologies along with their framework standards that can be employed for SG [7]. Historically, Power Line Communication (PLC) provided broadband Internet access to residential customers, connectivity within an office, industry, home, etc. The BB-PLC technology is adept at command and control for automation and remote metering. The basic motivation for utilizing PLC in SG infrastructure is its cost-effectiveness since other wireless or wired technology could be very expensive [8].

However, challenges arise when using standard PLC MODEMs designed for home users for data transmission within the SG context. Limitations and problems that barricade communication are discussed by authors in [9]. The research study further highlights the opportunity of transmission and discusses the probable solutions to these challenges including the application of pulse width modulation filters to minimize these problems. In [10], researchers discuss the requirement of communication network and transmission concepts for usage of the already existing power transmission and distribution infrastructure resources in order to fulfill these requirements. In [11], researchers presented a summary of Distribution Line Carrier (DLC), highlighting the methods of testing, integration and verification of PLC technologies and IP communication for utilities. Bluetooth is a cost-effective wireless communication device, widely utilized in SG communication for observing the energy usage of a single module or in an Individual Area Network (IAN). Bluetooth is particularly useful for controlling changes, such as switches, within a Small Area Network (SAN). Its low power consumption makes it appropriate

for transmission in a Personal Area Network (PAN) within a radius of 10 meters. The data speed of Bluetooth is 3 Mbps and line of sight for connection is not required [12].

Moreover, Zigbee is another economical device in terms of power efficiency and cost effectiveness. It is suitable inside home environments or HAN applications of SG communication and it can offer better coverage as compared to Bluetooth connection. Zigbee is highly affective for monitoring of automatic lightning, performance of automatic metering and energy consumption of individual load connected at home. Its low power consumption leads to an extended battery life within a range of 10 meters. It offers low data rates of 20-250 Kbps as compared to Bluetooth connection [12]. Wi-Fi plays a crucial role in Smart Grid (SG) communication, primarily within Local Area Networks (LANs) for broadband Internet access. Wi-Fi technologies are used for automatic oversight and monitoring of energy utilization in diverse local areas. Due to the available support of mesh networking, Wi-Fi technologies permit communication among NAN in SG and can support a distance of up to 250 m and a speed of 54 Mbps [13].

Worldwide Interoperability for Microwave Access (WiMAX) technology has several advantages over networking techniques including low cost of deployment, long network span seamless communications, scalability, appropriate bandwidth, robust security protocols, and high data rates. WiMAX is suitable for wireless meter reading in AMI as it can be used to construct a real-time automated costing scheme built on real-time energy utilization. Furthermore, reliable and secure transmission can be made possible by utilizing WiMAX for fast restoration and detection of outages enabling fast power transfer and distribution reliability. Additionally, its adaptive modulation technique improves Signal-to-Noise Ratio (SNR), making it effective even in low channel conditions with minimal Received Signal Strength (RSS) [14]. Cellular communication technology has been used as the backbone of SG communication, generally in power substations/stations at a distance far from consumers of rural and urban areas. These consumers generate substantial datasets, including meter readings, sensor data, and electrical parameters. In such circumstances, cellular communication technologies provide widespread coverage, high data rates, and 100% deployment in urban and rural areas. In [15], the authors provided a comprehensive survey of the usage of GPRS, UMTS, GSM, and WCDMA technologies by various companies for SG communication, highlighting the widespread adoption and benefits of cellular technology, including enhanced data security, authentication, and cost-effective deployment.

A multi-path channel model is essential for multiple WANs to increase spectral efficiency and to find the optimum number of mesh clients which can concurrently utilize the channel. Authors in [16] showed that a wireless network is designed for SG using OFDMA, which offers enhanced efficiency and better performance in multi-path channels. The authors in [17] assert that the adoption of 4G/LTE technology, known for its IP-based broadband capabilities, is suitable for advancing information and communication technologies and distributed electric power networks within Smart Grid (SG) infrastructure. Satellite Communication (SATCOM) systems are independent of distance covered and scalability, expand seamlessly with coverage area making satellite communication appropriate for deployments over WAN. Utilization of satellite communication system in SG is theoretically possible but it requires more investigation and refinement [18]. One of the research areas is to optimize SATCOM for SG in LEO systems which offers a strong potential to implement future networks.

Noise in SG Communication System:

Figure 1 shows an SG communication system where a Grid Station (GS) acts as a BS and transmits data to SMs and User Equipment (UE).

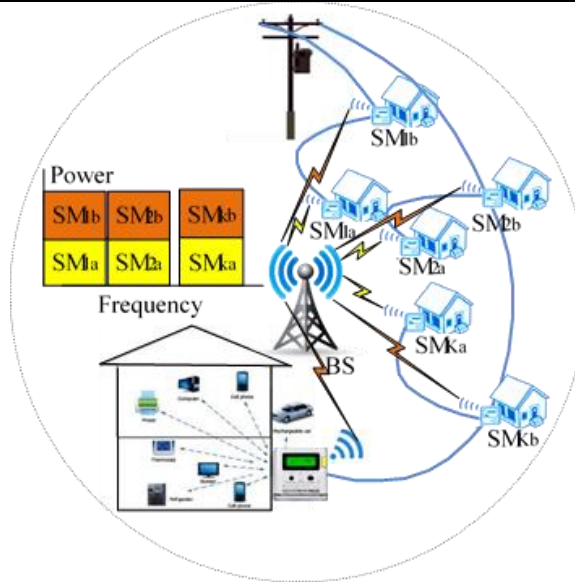


Figure 1: SG Communication System

BS utilizes power division NOMA scheme for SMs which sufficiently distant from each other in order to implement NOMA. BS allocates access through the OFDMA scheme to SMs at the same distance from BS because NOMA is not applicable to these SMs. Furthermore, SMs are part of the electric grid and are affected by a high-voltage electromagnetic disturbance that creates impulses at SMs. Therefore, the performance of the communication link is degraded by impulse noise.

For the downlink NOMA system, input BPSK information signals 's' with average energy E_b ($s_1 = \sqrt{E_b}$ or $s_0 = -\sqrt{E_b}$ with equal a priori probabilities) is transmitted over the channel with combined noise amplitude ' ξ ' of impulsive noise and Additive White Gaussian Noise (AWGN). BS transmits two or more data streams concurrently in the same frequency and time slot. Before transmission, the parallel data for different SMs are encoded and modulated by utilizing BPSK modulation in the DAC unit. Then, data of different SMs is summed up to generate a superposed signal. On the receiver side, SIC is employed to demodulate and decode the received superposition signals. Furthermore, the Rayleigh fading channel which is contaminated by impulse noise is considered in SG applications. Also, Perfect Channel State Information (CSI) is considered to be available. The received symbol for i_{th} SM in the presence of impulse noise SMi can be written as:

$$r_i = s_i h_i + \chi + \xi \quad (1)$$

Where h is the fading channel coefficient, χ is the level of inter-cell interference and ξ is the average combined (background noise and Impulsive noise) noise level.

Impulse Noise Models:

The channels used in SG communication are a combination of impulsive noise and background noise. As compared to background noise, impulsive noise changes more quickly with time. Therefore, a combined statistical noise model is required to include the consequence of both background noise and impulsive noise. Bernoulli-Gaussian model and Laplacian-Gaussian model are the most suitable models used in literature for combined noise scenario [19][20].

Bernoulli-Gaussian Model:

The level of noise can be represented using the Bernoulli-Gaussian model:

$$\xi = n_G + b n_I \quad (2)$$

Where b is the arrival rate of impulsive noise with portability of p , independent of n_G and n_I for Bernoulli random sequence. Also, n_G and n_I are the Additive White Gaussian Noise

(AWGN) with mean zero and variance σ_G^2 and σ_I^2 , respectively [19]. The noise is made up of i.i.d. random variables with p.d.f. and is expressed as follows:

$$P_n(x) = (1 - p)\mathbf{G}(x, 0, \sigma_G^2) + p\mathbf{G}(x, 0, \sigma_G^2 + \sigma_I^2) \quad (3)$$

Where $\mathbf{G}(v, 0, \sigma_G^2)$ is a Gaussian pdf with mean μ_x and variance σ_x^2 . ξ_0 is the average noise power, which is expressed as follows:

$$\xi_0 = E[n^2] \quad (4)$$

$$\xi_0 = E[n_G^2] + E[b^2]E[n_I^2] \quad (5)$$

$$\xi_0 = \sigma_G^2 + p\sigma_I^2 \quad (6)$$

Laplacian-Gaussian Model:

According to the Laplacian-Gaussian noise model whose PDF has a heavier tail with zero mean and variance $2c^2$, the average noise power can be written as:

$$\xi_0 = E[n_G^2] + E[r^2]E[n_I^2] \quad (7)$$

$$\xi_0 = \sigma_G^2 + p2c^2 \quad (8)$$

Where r is the impulsive noise arrival rate, characterized as a Bernoulli random variable with a probability of p : [20].

Proposed NOMA Scheme:

In non-orthogonal downlink transmission for SG, GS/BS sends signals to several SMs at the same time and frequency. Each SM uses a percentage of total power, numerous SMs can share the same frequency bandwidth while being distinguishable by the power level assigned by the GS. The decoder recognizes SM signals through the SIC scheme, while other SM signals are handled as noise [21]. The received symbol for i^{th} SM in the presence of impulse noise SM_i can be written as:

$$r_i = s_i h_i + \sum_{j=1, j \neq i}^{i-1} s_j h_i + \xi \quad (9)$$

In NOMA, user signals close to the BS are considered interference, whereas user signals further away from the BS are considered noise. Where in eq (9) the second term $\chi = \sum_{j=1, j \neq i}^{i-1} s_j h_i$ represents the level of inter-cell interference symbols for SM_i . $\chi_0 = \sum_{j=1, j \neq i}^{i-1} \alpha_j P |h_i|^2$ represents the average power of inter-cell interference, which is considered as noise. P is the total power for all UEs/SMs. α is the power allocation coefficient, $\alpha_1 + \alpha_2 + \alpha_3 + \dots + \alpha_i = 1$ and h is the fading coefficient of the wireless channel [4]. Now the above equation becomes:

$$r_i = s_i h_i + \chi + \xi \quad (10)$$

The channel is considered a Rayleigh fading channel. The probability density function (pdf) of the Rayleigh fading channel with random variable $v = h$ is given by:

$$f_h(v) = \frac{v}{\sigma_h^2} \exp\left(\frac{-v^2}{2\sigma_h^2}\right) \quad (11)$$

and its m^{th} moment is:

$$E[h^m] = (2\sigma_h^2)^{m/2} \Gamma\left(\frac{m}{2} + 1\right) \quad (12)$$

The average received SNR is defined as:

$$\bar{\gamma} = E[\gamma] = \frac{\alpha_i E_b E[h^2]}{\chi_0 + \xi_0} \quad (13)$$

If γ is the instantaneous output SNR:

$$\gamma = \frac{\alpha_i E_b h_i^2}{\chi_0 + \xi_0} \quad (14)$$

$|h|^2$ is chi-square distributed with the constraint that $|h|$ is Rayleigh distributed through two degrees of freedom. If $|h|^2$ is chi-square distributed, then γ is also

$$f(\gamma) = \frac{1}{\bar{\gamma}} \exp^{\frac{\gamma}{\bar{\gamma}}}, \bar{\gamma} > 0 \quad (15)$$

The probability density function of Rayleigh fading channel with random variable $u = h^2$ can be written as:

$$f_\gamma(u) = \frac{1}{\left(\frac{\alpha_i E_b}{\chi_0 + \xi_0}\right)} \exp\left(\frac{\left(\frac{\alpha_i E_b u \gamma}{\chi_0 + \xi_0}\right)}{\left(\frac{\alpha_i E_b}{\chi_0 + \xi_0}\right)}\right) \quad (16)$$

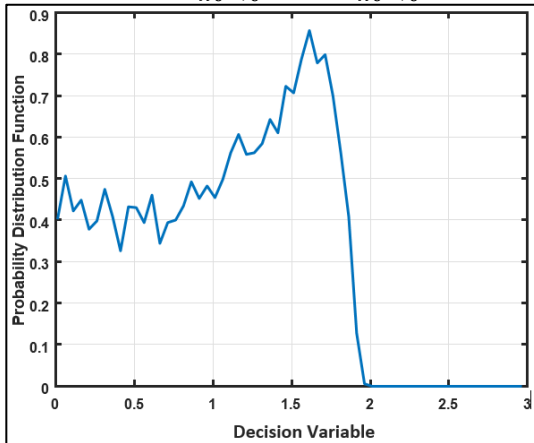


Figure 2: PDF of SNIR

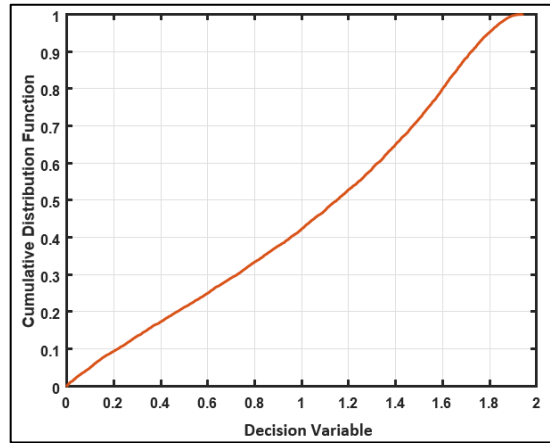


Figure 3: CDF of SNIR

Figure 2 and Figure 3 are the results of an analytical framework for estimating significant statistical metrics, PDF and CDF of instantaneous SNR. The analysis is based on appropriate expressions extracted for the NOMA downlink system, where the SIC receiver operates over Rayleigh fading channels with impulse noise and interference of other user signals. The achieved result specifies that a combination of interference and fading seriously affects the performance of the system. Furthermore, obtained expressions are applied to investigate the performance of the NOMA system, in terms of the average bit error probability.

Derivation of Bit Error Rate Equation:

The BER is given by:

$$P_e = \int_0^\infty P_e(e/u) f_\gamma(u) du \quad (17)$$

The BER $P(e | \cdot)$ depends on γ . Considering the instantaneous SNR (γ), pdf of r depends on h^2 and s and can be derived from (3) and (9) as follows:

$$p(r | h^2, s_0) = \frac{1-p}{\sqrt{\pi(\chi_0 + 2\sigma_G^2)}} \exp\left(\frac{-(r + \sqrt{h^2 \alpha E_b})}{\chi_0 + 2\sigma_G^2}\right) + \frac{p}{\sqrt{\pi(\chi_0 + 2\sigma_G^2 + 2\sigma_I^2)}} \exp\left(\frac{-(r + \sqrt{h^2 \alpha E_b})}{\chi_0 + 2\sigma_G^2 + 2\sigma_I^2}\right) \quad (18)$$

$$p(r | h^2, s_1) = \frac{1-p}{\sqrt{\pi(\chi_0 + 2\sigma_G^2)}} \exp\left(\frac{-(r - \sqrt{h^2 \alpha E_b})}{\chi_0 + 2\sigma_G^2}\right) + \frac{p}{\sqrt{\pi(\chi_0 + 2\sigma_G^2 + 2\sigma_I^2)}} \exp\left(\frac{-(r - \sqrt{h^2 \alpha E_b})}{\chi_0 + 2\sigma_G^2 + 2\sigma_I^2}\right) \quad (19)$$

$$p(r | h^2, s_i) = \frac{1-p}{\sqrt{\pi(\chi_0 + 2\sigma_G^2)}} \exp\left(\frac{-(r - \sqrt{h^2 \alpha E_b})}{\chi_0 + 2\sigma_G^2}\right) + \frac{p}{\sqrt{\pi(\chi_0 + 2\sigma_G^2 + 2\sigma_I^2)}} \exp\left(\frac{-(r - \sqrt{h^2 \alpha E_b})}{\chi_0 + 2\sigma_G^2 + 2\sigma_I^2}\right) \quad (19)$$

The conditional BER which depends on γ , when the transmitted symbol $s_i, i = 0, 1$, is received as:

$$P(e | h^2, s_i) = \frac{1}{2}(1-p)Q\left(\sqrt{\frac{h^2 \alpha E_b}{\chi_0 + 2\sigma_G^2}}\right) + \frac{1}{2}pQ\left(\sqrt{\frac{h^2 \alpha E_b}{\chi_0 + 2\sigma_G^2 + 2\sigma_I^2}}\right) \quad (20)$$

The conditional BER which depends on γ can be written as:

$$P(e | \gamma) = P(e | h^2, s_0) = P(e | h^2, s_0) \quad (21)$$

$$P(e | \gamma) = \frac{1}{2}(1-p)Q\left(\sqrt{\frac{h^2\alpha E_b}{\chi_0 + 2\sigma_G^2}}\right) + \frac{1}{2}pQ\left(\sqrt{\frac{h^2\alpha E_b}{\chi_0 + 2\sigma_G^2 + 2\sigma_I^2}}\right) \quad (22)$$

$$P_e = \int_0^{\infty} \left\{ (1-p) \frac{\chi_0 + 2\sigma_G^2}{\alpha_i E_b} Q\left(\sqrt{\frac{h^2\alpha E_b}{\chi_0 + 2\sigma_G^2}}\right) \exp^{u_\gamma} + p \frac{\chi_0 + 2\sigma_G^2 + 2\sigma_I^2}{\alpha_i E_b} Q\left(\sqrt{\frac{h^2\alpha E_b}{\chi_0 + 2\sigma_G^2 + 2\sigma_I^2}}\right) \exp^{u_\gamma} \right\} d\gamma \quad (23)$$

The first part of eq (23) can be written as:

$$P_e = \frac{1}{\left(\frac{\alpha E_b}{\chi_0 + 2\sigma_G^2}\right)} \int_0^{\infty} Q\left(\sqrt{\frac{h^2\alpha E_b}{\chi_0 + 2\sigma_G^2}}\right) \exp\left(\frac{\left(\frac{\alpha E_b h^2}{\chi_0 + 2\sigma_G^2}\right)}{\left(\frac{\alpha E_b}{\chi_0 + 2\sigma_G^2}\right)}\right) d\gamma \quad (24)$$

$$P_e = \frac{1}{2\bar{\gamma}} \int_0^{\infty} Q(\sqrt{\gamma}) \exp\left(-\frac{\gamma}{\bar{\gamma}}\right) d\gamma \quad (25)$$

$$P_e = \frac{1}{2\bar{\gamma}} \left[Q(\sqrt{\bar{\gamma}}) (-\bar{\gamma}) \exp\left(-\frac{\bar{\gamma}}{\bar{\gamma}}\right) \Big|_0^{\infty} - \int_0^{\infty} (-\bar{\gamma}) \exp\left(-\frac{\bar{\gamma}}{\bar{\gamma}}\right) \frac{-1}{\sqrt{\pi}} \exp(-\gamma) \gamma^{-1/2} d\gamma \right] \quad (26)$$

Where;

$$Q(\sqrt{x}) = \frac{1}{\sqrt{\pi}} \int_x^{\infty} e^{-t} t^{-1/2} dt$$

$$\frac{dQ(\sqrt{x})}{dx} = \frac{-1}{\sqrt{\pi}} e^{-x} x^{-1/2}$$

$$P_e = \frac{1}{2\bar{\gamma}} \left[-\bar{\gamma} Q(\sqrt{\bar{\gamma}}) \exp\left(-\frac{\bar{\gamma}}{\bar{\gamma}}\right) \Big|_0^{\infty} - \frac{\bar{\gamma}}{\sqrt{\pi}} \int_0^{\infty} \exp\left[-\gamma\left(\frac{\bar{\gamma}+1}{\bar{\gamma}}\right)\right] \gamma^{-1/2} d\gamma \right] \quad (27)$$

$$\int_0^{\infty} \exp\left[-\gamma\left(\frac{\bar{\gamma}+1}{\bar{\gamma}}\right)\right] \gamma^{-1/2} d\gamma$$

$$= \int_0^{\infty} \exp(-u) \left(\frac{\bar{\gamma}}{\bar{\gamma}+1}\right) u^{-1/2} \left(\frac{\bar{\gamma}}{\bar{\gamma}+1}\right) du$$

$$= \left(\frac{\bar{\gamma}}{\bar{\gamma}+1}\right)^{1/2} \int_0^{\infty} \exp(-u) u^{-1/2}$$

$$= \sqrt{\pi} \sqrt{\frac{\bar{\gamma}}{\bar{\gamma}+1}} Q(\sqrt{u}) = \sqrt{\pi} \sqrt{\frac{\bar{\gamma}}{\bar{\gamma}+1}} Q\left(\sqrt{\frac{\bar{\gamma}+1}{\bar{\gamma}}}\sqrt{\bar{\gamma}}\right) \quad (28)$$

Now eq (26) becomes:

$$P_e = \frac{1}{2\bar{\gamma}} \left[-\bar{\gamma} Q(\sqrt{\bar{\gamma}}) \exp\left(\frac{\bar{\gamma}}{\bar{\gamma}}\right) - \bar{\gamma} \sqrt{\frac{\bar{\gamma}}{\bar{\gamma}+1}} Q\left(\sqrt{\frac{\bar{\gamma}+1}{\bar{\gamma}}}\sqrt{\bar{\gamma}}\right) \right]_0^{\infty} \quad (29)$$

$$P_e = \frac{1}{2} \left(1 - \sqrt{\frac{\bar{\gamma}}{\bar{\gamma}+1}} \right) \quad (30)$$

$$P_e = \frac{1}{2} \left(1 - \sqrt{\frac{\alpha E_b}{\alpha E_b + \chi_0 + 2\sigma_G^2}} \right) \quad (31)$$

Similarly, the second part of eq (23) can be written as:

$$P_e = \frac{1}{\left(\frac{\alpha E_b}{\chi_0 + 2\sigma_G^2 + 2\sigma_I^2}\right)} \int_0^{\infty} Q\left(\sqrt{\frac{h^2\alpha E_b}{\chi_0 + 2\sigma_G^2 + 2\sigma_I^2}}\right) \exp\left(\frac{\left(\frac{\alpha_i E_b h^2}{\chi_0 + 2\sigma_G^2 + 2\sigma_I^2}\right)}{\left(\frac{\alpha E_b}{\chi_0 + 2\sigma_G^2 + 2\sigma_I^2}\right)}\right) d\gamma \quad (32)$$

$$P_e = \frac{1}{2} \left(1 - \sqrt{\frac{\alpha E_b}{\alpha E_b + \chi_0 + 2\sigma_G^2 + 2\sigma_I^2}} \right) \quad (33)$$

From eq (23), we can express the integral form of the BER as follows:

$$P_e = \frac{1}{2}(1-p)\left(1 - \sqrt{\frac{\alpha E_b}{\alpha E_b + \chi_0 + 2\sigma_G^2}}\right) + \frac{1}{2}p\left(1 - \sqrt{\frac{\alpha E_b}{\alpha E_b + \chi_0 + 2\sigma_G^2 + 2\sigma_I^2}}\right) \quad (34)$$

NOMA SE-EE Trade-off in Presence of Impulse Noise:

For the SE-EE trade-off, consider two user model for NOMA and OFDMA. Their achievable data rates can be expressed as:

$$R_1 = B \log_2 \left(1 + \frac{p_1 g_1}{\xi}\right) \quad (35)$$

$$R_2 = B \log_2 \left(1 + \frac{p_2 g_2}{p_1 g_2 + \xi}\right) \quad (36)$$

Therefore, the sum rate can be expressed as:

$$R = B \left\{ \log_2 \left(1 + \frac{p_1 g_1}{\xi}\right) + \log_2 \left(1 + \frac{p_2 g_2}{p_1 g_2 + \xi}\right) \right\} \quad (37)$$

Where p_1, g_1 and p_2, g_2 are power and channel gains of SM1 and SM2 respectively and ξ is combined noise. The total power consumed at the receiver is P and can be written as;

$$P = P_t + P_c + P_{SIC} \quad (38)$$

Where $P_t = \sum_{k=1}^K \alpha_k P$ is the true transmitting power consumed, P_c is the constant power consumption of the circuit, P_{SIC} is the SIC power consumption for one iteration and $P_{SIC} = \sum_{i=1}^{K-1} P_{i(SIC)}$ is the total power consumed to perform SIC computation. Energy efficiency (bit/joule) for SM_k is given as:

$$EE = \frac{R}{BP} \quad (39)$$

$$EE = \frac{B \left\{ \log_2 \left(1 + \frac{p_1 g_1}{\xi}\right) + \log_2 \left(1 + \frac{p_2 g_2}{p_1 g_2 + \xi}\right) \right\}}{BP} \quad (40)$$

Spectral efficiency (bit/sec/Hertz) for SM_k is given as follows:

$$SE = \frac{R}{B} \quad (41)$$

$$SE = \frac{B \left\{ \log_2 \left(1 + \frac{p_1 g_1}{\xi}\right) + \log_2 \left(1 + \frac{p_2 g_2}{p_1 g_2 + \xi}\right) \right\}}{B} \quad (42)$$

Results and Discussion:

Limitations and Recommendations:

While the research demonstrates the effectiveness of NOMA in SG communication systems, several limitations need to be addressed. The study primarily focuses on theoretical models and simulations, which may not fully capture real-world complexities and variances in SG environments. The assumptions made for impulse noise characteristics might differ significantly from actual conditions, potentially affecting the accuracy of the results. Furthermore, the research does not thoroughly explore the impact of NOMA on latency, which is a critical parameter for many SG applications requiring real-time data processing and decision-making. Additionally, the study does not address the potential scalability challenges of implementing NOMA in large-scale SG networks, where the coordination and management of multiple users could become increasingly complex. Lastly, the data security implications of NOMA in SG communications are not discussed, leaving a gap in understanding how this technology affects data integrity and privacy.

To address these limitations, future research should include extensive field trials and real-world testing to validate the theoretical findings and adapt the models to practical scenarios. It is recommended to study the impact of NOMA on latency to ensure it meets the stringent requirements of real-time SG applications. Researchers should also investigate the scalability of NOMA, developing strategies to manage the complexity of user coordination in large networks. Furthermore, an in-depth analysis of the data security implications of NOMA is essential to ensure robust protection against potential cyber threats. Integrating machine learning techniques

to dynamically adapt to varying noise conditions and user demands could enhance the efficiency and reliability of NOMA-based SG communication systems.

Numerical simulations are performed to validate the derived close form of the BER equation. For this purpose, a typical NOMA downlink system is considered in which a single BS allocates power to different SMs. All SMs are equipped with signal antennas and a flat fading Rayleigh channel is considered for the link between each SM and BS.

Table 1: Simulation Parameters

No.	Parameters	Values
1	Number of SMs	$i, i \geq 2$
2	Available bandwidth, B	8.64MHz
3	Detection threshold of SIC receiver	10 dBm
4	Noise density at receiver, N_0	169dBm/Hz
5	Average impulse noise, N_I	$-30\text{dBm} \sim -35\text{dBm}$
6	Disturbance ratio, dr	0.00135, 0.00632, 0.0327
7	Number of antennas at each SM	1
8	Antenna gain at BS and SM	0dBm
9	Inter-site distance of NOMA users	0.6Km

The channel is considered a quasistatic channel therefore during transmission, channel characteristics remain the same. Since the performance of wireless channel for SMs is affected by impulse noise, average and instantaneous impulse noise level is considered in performance measuring metrics. The major simulation parameters and assumptions are taken from 3GPP LTE [22] and listed in Table 1.

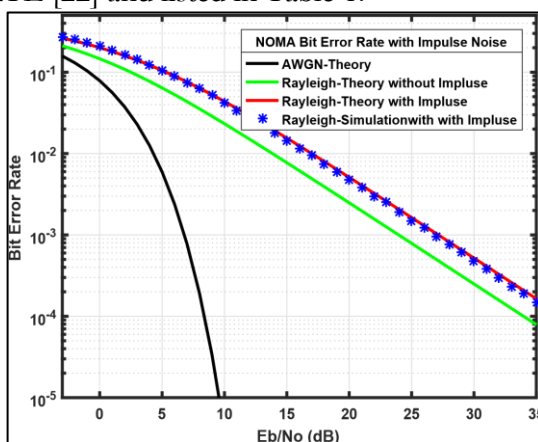


Figure 4: Average BER with impulse probability $p = 0.25$

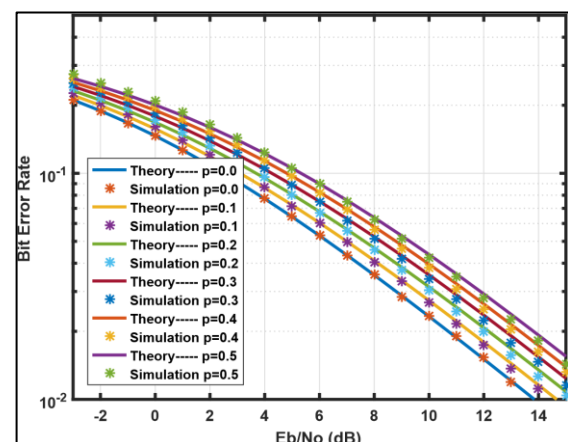


Figure 5: BER Theory and Simulation between $p = 0$ and $p = 0.5$

The deployment of accurate SNR level is essential in power based multiple access scheme for power allocation to different users. Figure 4 shows the comparison of the BER performance of AWGN and flat fading Rayleigh channel with impulse noise. The proposed model helps define the SNR level in the Rayleigh-Impulse channel for power allocation to SMs. It is observed from the Figure 4 that for a NOMA system in the Rayleigh fading channel, BER decreases rapidly with an increase in SNR. This occurs because different users' signals are superimposed and each user considers other user signals as noise. Therefore, increasing SNR increases fading in desired signal and as well as other user's signals. Moreover, Figure 4 shows a significant effect of impulse at low SNR. As the SNR increases, the effect of impulse noise decreases due to the low level of impulse between 0dB and 5dB. Therefore, there is a performance trade-off between impulse noise and fading.

The average BER of the NOMA system with the probability of impulse noise is illustrated in Figure 6. Plot shows the frequency of data transmission in the presence of impulse

noise with an impulse probability of p and Rayleigh fading. It is observed from the Figure 6 that increasing the probability of impulse, increases the SNR to maintain BER of the NOMA system constant. For a change in the probability of impulse by 0.1, there is a difference of about 1 dB in the SNR for the same value of BER. The higher the value of BER, the less affected it is by impulse noise compared to the low value of the BER. At 14 dB SNR, a change in the probability of impulse from 0.1 to 0.5 degrades BER from 0.01 to 0.02. The higher value of impulse noise (higher value of p) implies more degradation of the BER performance.

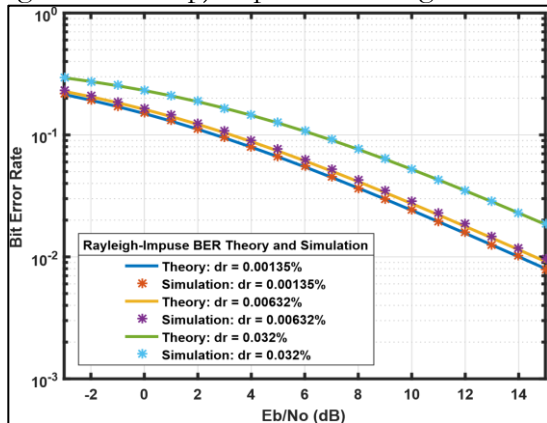


Figure 6: Average BER with probability of impulse with $dr = 0.00135\%$, $dr = 0.00632\%$ & $dr = 0.032\%$

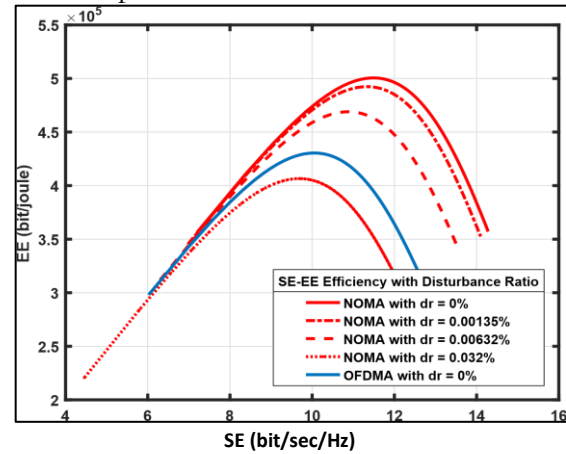


Figure 7: Spectral and energy efficiency trade-off in presence of impulse noise

The instantaneous value of impulse does not define the actual loss, as impulses occurs for a very short period and increases the level of noise up to 5dB, disappearing thereafter.

Therefore, it is defined by disturbance ratio $dr = \frac{\sum_{i=1}^l t_{w,i}}{T_{total}}$, where $t_{w,i}$ is the width of i_{th} impulse in a sec and l is the total number of impulses occurring in time $T_{tot}(\text{sec})$ [4].

Figure 6 illustrates a comparison of the BER performance of the NOMA system for three impulsive noise scenarios termed as heavily disturbed, medium disturbed and weakly disturbed. Signal power selection in NOMA is crucial because NOMA utilizes power domain multiple access technology. Any ambiguity in power selection affects SIC decoding since SIC decodes the desired signal from a superimposed signal based on its power difference. The demonstrated results are helpful in relevant real-life impulse scenarios for acceptable BER values.

Furthermore, Figure 7 illustrates the trade-off between spectral and energy efficiencies in the presence of impulse noise. The graph reveals an inverse relationship between disturbance ratio (dr) and the optimal trade-off. NOMA performs better with average impulse noise ($dr = 0.00632$) than OFDMA without impulse noise because all NOMA users utilize the same spectrum and are differentiated by their power level. Therefore, the peak value of NOMA with impulse noise is much higher than OFDMA without impulse noise.

The analysis of BER across different SNRs and impulse noise probabilities elucidates critical insights. Figure 4 portrays a discernible relationship between BER and SNR, emphasizing the necessity for optimal power allocation to counteract the adverse effects of fading and impulse noise. This aligns with previous NOMA studies [23] but highlights its superiority in spectral efficiency and reliability compared to conventional multiple access schemes like OFDMA. The impact of impulse noise, as depicted in Figure 5, underscores the imperative of higher SNR requirements to maintain a constant BER in noise-laden environments, and fill the gap in existing literature [24] on noise mitigation challenges in wireless communications. Furthermore, the examination of BER performance under varying disturbance ratios (Figure 6) accentuates the sensitivity of NOMA systems to impulse noise, necessitating robust error

correction mechanisms that are not addressed in [25]. The trade-off analysis between spectral and energy efficiencies in the presence of impulse noise (Figure 7) elucidates NOMA's superiority in leveraging spectrum resources, enhancing overall system efficiency even under average impulse noise conditions compared to OFDMA. Overall, these findings advocate for the suitability of NOMA in SG applications, offering a robust communication framework resilient to impulse noise and fading effects. This research lays a solid foundation for future endeavors in optimizing power allocation and developing advanced noise mitigation strategies to further enhance the reliability and efficiency of SG communication networks.

Strengths and Weaknesses:

The research presents several strengths, including its innovative integration of NOMA with SG communications, which addresses a crucial need for more efficient bandwidth usage and noise management. The study provides comprehensive mathematical models for Rayleigh fading and impulse noise, contributing to a deeper understanding of these phenomena in SG environments. Its focus on real-world challenges, such as impulse noise in SG communications, enhances the practical relevance of the findings, potentially leading to more reliable and efficient SG systems. Additionally, the derivation of closed-form equations for BER and SNR offers clear and quantifiable performance metrics to evaluate and optimize NOMA performance in the SG environment, emphasizing the resilience of NOMA against impulse noise. However, the research also has some weaknesses. It might rely on assumptions and simplifications in its models, which could limit the applicability of the findings to more complex real-world scenarios. Practical implementation of NOMA in existing SG infrastructures may face challenges, including compatibility with current technologies and the need for significant upgrades. Moreover, while the study focuses on impulse noise and Rayleigh fading, other types of noise and interference in various SG environments may also need consideration. Lastly, the conclusions are largely based on theoretical models and simulations; thus, experimental validation in real-world SG systems would strengthen the findings and demonstrate practical feasibility.

The practical applicability of this research is significant for the development and optimization of SG communication systems. By demonstrating the effectiveness of NOMA in mitigating impulse noise and improving bandwidth efficiency, this study provides crucial insights for enhancing the reliability and robustness of SG networks. The closed-form equations for BER and SNR developed in this research offer practical tools for engineers to design SG communication systems that can better withstand noise interference. Additionally, the improved bandwidth utilization enabled by NOMA allows for more efficient data transmission, which is particularly beneficial in densely populated areas with limited spectrum resources. The scalability of NOMA further ensures that SG systems can expand to accommodate future growth, maintaining responsive and efficient operations. Overall, this research provides valuable solutions for enhancing SG communications, with direct implications for improving the performance and cost-effectiveness of smart grid infrastructure.

Conclusion:

This study contributes novel insights into the performance of NOMA systems within the context of SG communication, particularly in the presence of impulse noise. Through comprehensive modeling and analysis, the study reveals that NOMA holds promise for meeting the high bandwidth demands of SG applications, despite the challenges posed by impulsive noise in fading environments. By evaluating key performance metrics such as BER, this research demonstrates the robustness of NOMA under realistic SG conditions. Moreover, the comparison with existing studies highlights the unique contribution of this research in integrating NOMA and impulse noise analysis within the SG framework. The implications of these findings extend to the design and deployment of communication infrastructure in smart grids, offering valuable insights for enhancing reliability and efficiency. Moving forward, future

research should focus on optimization techniques for NOMA systems, adaptive algorithms for impulse noise mitigation, and real-world deployment scenarios to further advance the field of smart grid communication.

Acknowledgment: The manuscript has not been published or submitted to other journals previously.

Author's Contribution:

- Author 1 performed the experiment, and the experiment's calculations, and wrote the manuscript.
- Author 2 performed simulations, analyzed the data and contributed to the final version of the manuscript.
- Author 3, 4 and 5 revised the manuscript and contributed to the final version of the manuscript.

Conflict of Interest: Authors have no conflict of interest in publishing this manuscript in IJIST.

Project Details: Not applicable.

References:

- [1] A. H. Al-Badi, R. Ahshan, N. Hosseinzadeh, R. Ghorbani, and E. Hossain, "Survey of Smart Grid Concepts and Technological Demonstrations Worldwide Emphasizing on the Oman Perspective," *Appl. Syst. Innov.* 2020, Vol. 3, Page 5, vol. 3, no. 1, p. 5, Jan. 2020, doi: 10.3390/ASI3010005.
- [2] M. Hussain and H. Rasheed, "Communication Infrastructure for Stationary and Organized Distributed Smart Meters," 2019 2nd Int. Conf. Commun. Comput. Digit. Syst. C-CODE 2019, pp. 17–22, Apr. 2019, doi: 10.1109/C-CODE.2019.8681020.
- [3] A. E. Ibhaze, M. U. Akpabio, and T. O. Akinbulire, "A review on smart metering infrastructure," *Int. J. Energy Technol. Policy*, vol. 16, no. 3, pp. 277–301, 2020, doi: 10.1504/IJETP.2020.107019.
- [4] M. Hussain and H. Rasheed, "Performance of Orthogonal Beamforming with NOMA for Smart Grid Communication in the Presence of Impulsive Noise," *Arab. J. Sci. Eng.*, vol. 45, no. 8, pp. 6331–6345, Aug. 2020, doi: 10.1007/S13369-020-04457-Y/METRICS.
- [5] M. Jayachandran and C. Kalaiarasu, "Power-Domain NOMA for Massive Connectivity in Smart Grid Communication Networks," *Lect. Notes Electr. Eng.*, vol. 795, pp. 205–212, 2022, doi: 10.1007/978-981-16-4943-1_19.
- [6] M. Hussain and H. Rasheed, "Nonorthogonal multiple access for next-generation mobile networks: A technical aspect for research direction," *Wirel. Commun. Mob. Comput.*, vol. 2020, 2020, doi: 10.1155/2020/8845371.
- [7] A. Gopstein, A. Goldstein, D. M. Anand, and P. Boynton, "NIST Special Publication 1900-102 Summary Report on NIST Smart Grid Testbeds and Collaborations Workshops Summary Report on NIST Smart Grid Testbeds and Collaborations Workshops," 2019, doi: 10.6028/NIST.SP.1900-102.
- [8] J. A. Cortés and J. M. Idiago, "Smart Metering Systems Based on Power Line Communications," *Energy Syst. Electr. Eng.*, vol. Part F2127, pp. 121–170, 2019, doi: 10.1007/978-981-13-1768-2_4.
- [9] M. Orgon, M. Stefanicka, I. Schmidt, I. Zolotova, and D. Cupkova, "Testing home PLC network in multi-storey house," *Int. Congr. Ultra Mod. Telecommun. Control Syst. Work.*, vol. 2019-October, Oct. 2019, doi: 10.1109/ICUMT48472.2019.8970805.
- [10] S. Barker, D. Irwin, and P. Shenoy, "Pervasive Energy Monitoring and Control Through Low-Bandwidth Power Line Communication," *IEEE Internet Things J.*, vol. 4, no. 5, pp. 1349–1359, Oct. 2017, doi: 10.1109/JIOT.2017.2703916.
- [11] C. M and S. S, "A Survey on Narrow Band Power Line Carrier Communication for Efficient and Secure Data Transmission in Smart Grid Applications," Jun. 2021, doi: 10.4108/EAI.7-6-2021.2308770.
- [12] A. O. A. Alubodi, I. B. N. Al-Mashhadani, and D. S. S. Mahdi, "Design and Implementation

of a Zigbee, Bluetooth, and GSM-Based Smart Meter Smart Grid,” IOP Conf. Ser. Mater. Sci. Eng., vol. 1067, no. 1, p. 012130, Feb. 2021, doi: 10.1088/1757-899X/1067/1/012130.

[13] “A Spectrum Sharing based Metering Infrastructure for Smart Grid Utilizing LTE and WiFi - Advances in Science, Technology and Engineering Systems Journal.” Accessed: May 20, 2024. [Online]. Available: <https://www.astesj.com/v04/i02/p09/>

[14] R. Daryapurkar and R. G. Karandikar, “WIMAX Smart Grid Communication network for a Substation,” IFIP Int. Conf. Wirel. Opt. Commun. Networks, WOCN, vol. 2019-December, Dec. 2019, doi: 10.1109/WOCN45266.2019.8995127.

[15] C. Kalalas, L. Thrybom, and J. Alonso-Zarate, “Cellular Communications for Smart Grid Neighborhood Area Networks: A Survey,” IEEE Access, vol. 4, pp. 1469–1493, 2016, doi: 10.1109/ACCESS.2016.2551978.

[16] E. Shafter, A. Noorwali, and R. K. Rao, “OFDM systems with CPM mappers for smart grid applications,” 2015 IEEE Electr. Power Energy Conf. Smarter Resilient Power Syst. EPEC 2015, pp. 424–428, Jan. 2016, doi: 10.1109/EPEC.2015.7379988.

[17] H. Gozde, M. C. Taplamacioglu, M. Ari, and H. Shalaf, “4G/LTE technology for smart grid communication infrastructure,” 2015 3rd Int. Istanbul Smart Grid Congr. Fair, ICSG 2015, Dec. 2015, doi: 10.1109/SGCF.2015.7354914.

[18] A. Meloni and L. Atzori, “The Role of Satellite Communications in the Smart Grid,” IEEE Wirel. Commun., vol. 24, no. 2, pp. 50–56, Apr. 2017, doi: 10.1109/MWC.2017.1600251.

[19] H. V. Vu, N. H. Tran, T. V. Nguyen, and S. I. Hariharan, “Estimating Shannon and constrained capacities of Bernoulli-Gaussian impulsive noise channels in Rayleigh fading,” IEEE Trans. Commun., vol. 62, no. 6, pp. 1845–1856, 2014, doi: 10.1109/TCOMM.2014.2316267.

[20] S. Prakash, A. Bansal, and S. K. Jha, “Performance analysis of narrowband PLC system under Gaussian Laplacian noise model,” Int. Conf. Electr. Electron. Optim. Tech. ICEEOT 2016, pp. 3597–3600, Nov. 2016, doi: 10.1109/ICEEOT.2016.7755376.

[21] M. Hussain and H. Rasheed, “A Computational Power Allocation Scheme for Fair NOMA Downlink System,” J. Inf. Commun. Technol. Robot. Appl., pp. 73–79, Jun. 2018, Accessed: Apr. 19, 2024. [Online]. Available: <https://jictra.com.pk/index.php/jictra/article/view/83>

[22] G. A. Medina-Acosta et al., “3GPP Release-17 Physical Layer Enhancements for LTE-M and NB-IoT,” IEEE Commun. Stand. Mag., vol. 6, no. 4, pp. 80–86, Dec. 2022, doi: 10.1109/MCOMSTD.0001.2100099.

[23] B. Pavithra and P. Chakraborty, “Performance Analysis of Bit Error Rate, Capacity and Outage Probability using Power Domain Non-Orthogonal Multiple Access (PD-NOMA) and Orthogonal Multiple Access (OMA) with Far/Near User,” Proc. - 2022 6th Int. Conf. Intell. Comput. Control Syst. ICICCS 2022, pp. 166–170, 2022, doi: 10.1109/ICICCS53718.2022.9788438.

[24] Y. Jang, “Closed-form BER expression for multi-user downlink NOMA,” Phys. Commun., vol. 64, p. 102354, Jun. 2024, doi: 10.1016/J.PHYCOM.2024.102354.

[25] A. Al Hanif, A. M. T. Khel, and K. A. Hamdi, “BER Analysis of Multi-User NOMA Networks in the Presence of Interference,” IEEE Commun. Lett., 2024, doi: 10.1109/LCOMM.2024.3381496.



Copyright © by authors and 50Sea. This work is licensed under Creative Commons Attribution 4.0 International License.